Proceedings of the IASS 2024 Symposium
Redefining the Art of Structural Design
August 26-30, 2024, Zurich, Switzerland
Philippe Block, Giulia Boller, Catherine DeWolf,
Jacqueline Pauli, Walter Kaufmann (eds.)

Structural behaviour of concrete shells using brittle reinforcement materials: a case study on stay-in-place flexible formworks with integrated high-strength textiles

Minu LEE*

*schlaich bergermann partner
Brunnenstr. 110c, 13355 Berlin, Germany
m.lee@sbp.de

Abstract

Concrete shells with structurally informed geometries – i.e. anti-funicular shapes exhibiting predominantly compressive stresses under permanent loads – are highly efficient, allowing for minimal material use and reducing the amount of flexural reinforcement. However, their complex doubly curved geometry is usually associated with high cost and labour for the production of the formwork and erection of the scaffolding when applying conventional construction procedures.

A potential approach to overcome these challenges is the KnitCrete technology developed at ETH Zürich, which is a flexible formwork system based on weft-knitted textiles. Recent studies have explored the mechanical behaviour of integrating high-strength, non-corrosive textile rovings, its activation as a stay-in-place reinforcement, and its potential for material-efficient design of concrete structures. While the use of weft-knitted fabrics with integrated textile rovings extends the design spectrum of feasible concrete structures, the brittle nature of the reinforcement has significant implications on the design principles regarding the announcement of the upcoming failure and the redistribution of internal stresses.

This study investigates approaches for ensuring a ductile behaviour in concrete structures with brittle weft-knitted textile reinforcement. To this end, a parametric case study on various doubly curved shells is conducted, focusing on the structural behaviour regarding strength and deformation capacity. The results suggest that (i) a ductile failure may be achieved through the combination of brittle and ductile reinforcement, and (ii) an increasing degree of complexity in the geometry may lead to a pseudo-ductile behaviour due to progressive failure or cracking within the concrete shell.

Keywords: concrete shells, textile reinforcement, brittle materials, ductility, non-linear modelling, KnitCrete

1. Introduction

The reduction of the concrete volume used in the construction sector has become one of the critical drivers for developing new composite materials and structural typologies. While anti-funicular concrete shells are highly efficient regarding their structural performance and material use, this typology has been widely abandoned due to the labour-, cost-, and time-intensive construction procedures. A potentially more economic approach for concrete structures with complex geometries is the KnitCrete technology [1, 2]: weft-knitted textiles are tensioned in a scaffolding frame, additionally supported by cables or bending-active elements, and coated with a thin layer of fast-setting cement paste or epoxy resin, providing fast fabrication while reducing the amount of temporary support elements and waste from scaffolding and formworks. The author has further studied the integration of high-strength textile fibres in the fabric formworks and its activation as reinforcement in the final state [3], investigating

the mechanical behaviour under various loading conditions [4, 5, 6]. The experimental investigations showed that the integrated textile reinforcement was able to provide a stable post-cracking behaviour with good predictability of results using state-of-the-art approaches for the mechanical modelling and numerical simulations [7]. However, the implications of using brittle reinforcement materials on the structural behaviour include the reduction of strength due to higher partial safety factors, increased modelling uncertainty of the internal actions, and reduced robustness in statically indeterminate systems due to the inability to redistribute internal forces, stemming from the lack of ductility [8, 9]. The author has studied various means to implement ductility in the global response analogously derived from other building materials, such as timber or glass, allowing the formulation of design principles to achieve an adequate post-cracking behaviour of concrete structures with brittle reinforcement materials, which includes the introduction of ductile materials in the governing sections and elements to enable the application of capacity-based design methods [3]. Furthermore, the concept of pseudo-ductility mimics a ductile behaviour, i.e. decreasing stiffness with increasing load, through the progressive failure or cracking of components in statically indeterminate systems, which holds a limited energy dissipation potential but announces the upcoming collapse by exhibiting large deformations near the failure load. The approaches of pseudo-ductility rely on complex geometries with a high degree of robustness and static indeterminacy and the non-linear behaviour of reinforced concrete, whose potentials for a benign failure behaviour and challenges regarding the modelling and predictability of the results are shown in the following.

2. Structural behaviour of concrete shells with brittle reinforcement

This section presents a case study focusing on the analysis of the non-linear load-deformation behaviour of curved concrete shells, highlighting the aspects regarding the implementation of ductility by means of ductile connections and pseudo-ductility from progressive cracking and failure of components.

2.1. Definition and parametrisation of shell geometry

The examined design is a shell bridge with a span of 12 m and a width of 2 m with fixed ends to increase the global stiffness and the degree of static indeterminacy, see Figure 1a. The slenderness of the arch, i.e. the ratio of the rise (h) to the span (l), along the centre axis of the shell is fixed at 1/10. The vertical alignment in the longitudinal direction is defined as a catenary following from the force and form diagram, illustrated in Figure 1b, considering the variable thickness (t), which linearly increases from 40 mm at the crown to 80 mm at the abutments. The degree of double curvature – represented by the Gaussian curvature K – is controlled by the shape of the middle section of the shell, which is defined as a parabola and results in anticlastic ($K < 0$), monoclastic ($K = 0$), and synclastic ($K > 0$) shell geometries, as shown in Figure 1c, 1d, and 1e, respectively.

2.2. Modelling assumptions and structural analysis

The non-linear finite element analysis is conducted with the commercial software *SOFiSTiK 2022* using the *Rhino/Grasshopper* interface for the parametric definition of the geometry, reinforcement properties, and structural analysis processes. The material behaviour is defined through the stress-strain relationships defined in Figure 2a-c. The structural geometry is translated from the parametric surface definition in Grasshopper to quad shell elements with a maximum mesh size of 300 mm. The textile reinforcement is modelled as an orthogonal grid of rovings with zero concrete cover, see Figure 2d. The reinforcement area in one layer is constant throughout the shell and is varied from 22.2 to 77.8 mm^2/m for various shells (local bending resistances corresponding to two and seven times the cracking moment

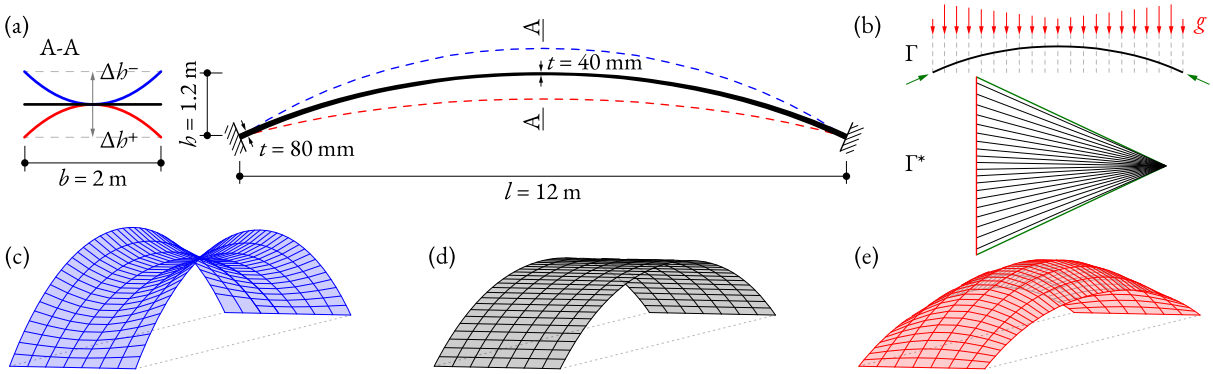

Figure 1: Vaulted shell structures: (a) parametric definition of geometry and static system; (b) anti-funicular geometry of the arch along the shell's centre axis following the form (Γ) and force (Γ*) diagrams under dead load; (c) anticlastic ($\Delta h/h < 0$), (d) monoclastic ($\Delta h/h = 0$), and (e) synclastic ($\Delta h/h > 0$) shell geometries.

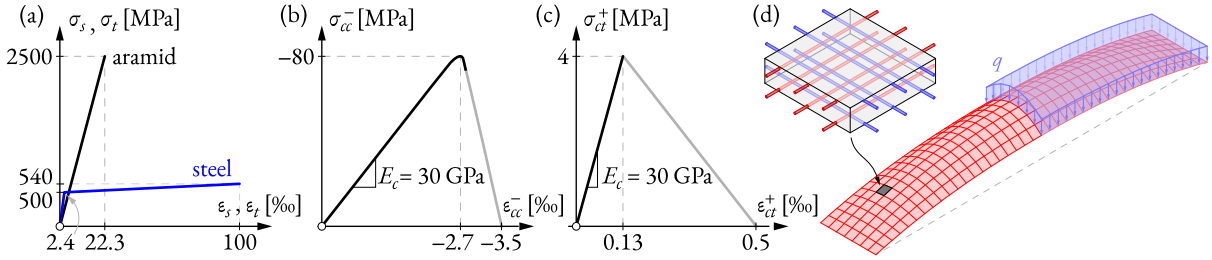

Figure 2: Modelling assumptions in numerical simulations: stress-strain relationships for material models for (a) textile and steel reinforcement, (b) concrete in compression, and (c) concrete in tension; (d) reinforcement layout; (e) element mesh and applied transient load.

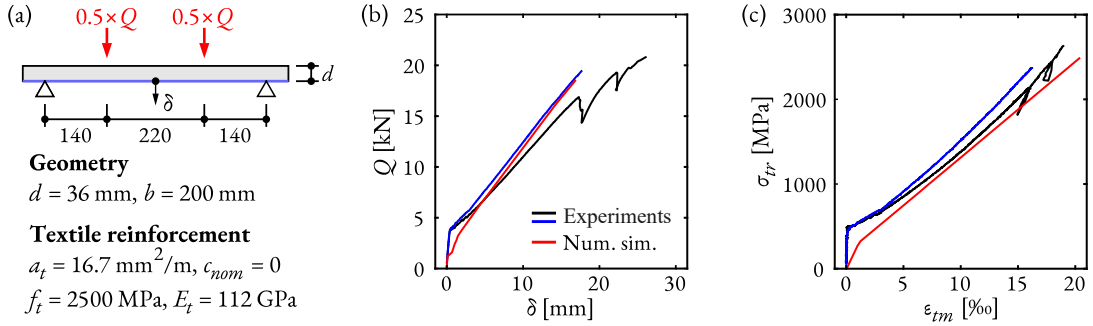

Figure 3: Validation of numerical simulations with four-point bending experiments [10]: (a) test setup, specimen dimensions, and reinforcement configuration; (b) total load vs mid-span deflection; (c) textile stress vs mean strains in constant moment zone.

of the thinnest section, respectively). Besides the self-weight, a transient load is applied on half of the surface of the structure. The load-deformation behaviour is simulated by progressively increasing the live load, considering the non-linear behaviour of the composite cross-section due to the decompression and cracking of the concrete. The material failure criteria are either reaching the strain limits of the reinforcement ($\varepsilon_{tu} = 22.3‰$) or the concrete ($\varepsilon_{cu} = -3.5‰$). The quality of the modelling approach is validated with corresponding bending tests from [10], which shows generally good agreement regarding the post-cracking behaviour, including the tension stiffening effect and the failure load, see Figure 3b-c.

2.3. Non-linear response of reinforced concrete shells

The structural behaviour of the concrete shells is investigated regarding their load-displacement relationship and their internal force, stress, and strain distribution, examining the geometry, reinforcement ratio, and specific material properties to identify the governing parameters.

2.3.1. Influence of curvature on the load-bearing behaviour

Figure 4a shows the load-displacement relationships of several shells with the lowest amount of textile reinforcement (a_t = 22.2 mm^2/m), varying the degree of double curvature. The load Q corresponds to the sum of the transient loads applied on half of the shell's surface, as described in Section 2.2.. The vertical deflections are taken at the quarter length of the span from the right abutment along the centre axis of the shell.

The introduction of double curvature to the shell geometry proves to be a decisive factor in increasing the cracking load, the post-cracking stiffness, and the ultimate strength. The rupture of the textile reinforcement governs the failure in all shells but the synclastic shell with the largest positive Gaussian curvature (Figure 4b), where the strain limit of the concrete is reached. The deflections at failure drastically decrease with an increasing degree of double curvature (Figure 4c), whereby synclastic shells generally lead to a stiffer behaviour. Figure 5 examines various characteristic states along the load-deformation curve of the single curved shell (Figure 5a), showing that the structure mainly behaves as a one-way arch. After initial cracking ('A'), the cracked regions in the longitudinal direction of the shell progressively grow until the failure occurs, as shown in Figure 5b. The compressive membrane forces (Figure 5c) remain fairly constant during the post-cracking phase ('B') with negligible tensile forces, while the bending moments continuously increase (Figure 5d). The activation of the tensile reinforcement (Figure 5e) consequently follows from the bending moments with the eventual failure due to reaching the tensile strength in the lower layer in the x-direction at the left abutment ('C'). In contrast, the anticlastic (Figure 6) and synclastic (Figure 7) shells exhibit a more complex cracking behaviour, with large regions where the sections exceed the tensile strength in both longitudinal and transverse directions. The curved middle sections allow the shells to carry the loads via membrane forces – forming pairs of tensile and compressive forces (Figure 6c and Figure 7c) – rather than local bending moments, significantly increasing the global strength and stiffness. The activation of the reinforcement in the top and bottom layers of the cross-section is, therefore, more uniformly distributed over the shell structures, see Figure 6e and Figure 7e, guaranteeing a more efficient utilisation of the material's strength.

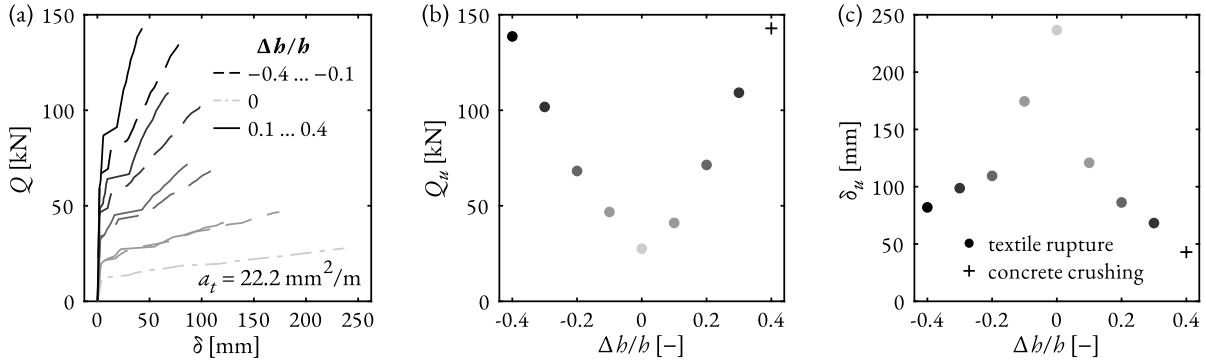

Figure 4: Influence of double curvature on the load-bearing behaviour (a_t = 22.2 mm^2/m): (a) load vs deflection; (b) ultimate load vs degree of double curvature; (c) deflection at ultimate load vs degree of double curvature.

2.3.2. Cracked pseudo-ductility

Due to the double curvature, the progressive cracking behaviour in compression-dominant concrete structures may result in a pseudo-ductile behaviour, which is dependent on the shell geometry. The variation of the double curvature leads to different behaviours in the transition from the uncracked to the fully cracked state regarding the increase of the loads and deformations, which can serve as measures for the pseudo-ductility. Note that a higher degree of double curvature does not necessarily result in

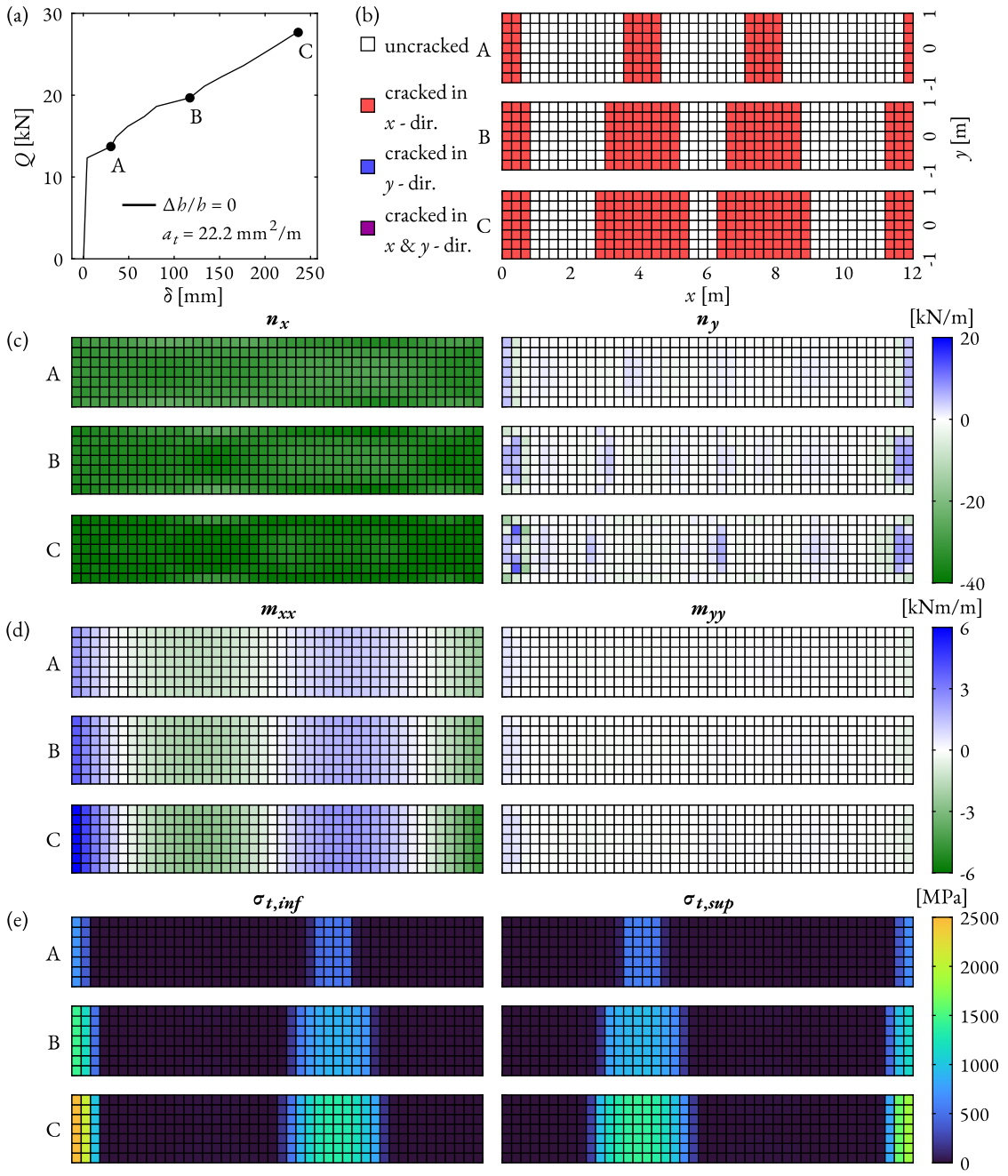

Figure 5: Load-deformation behaviour of monoclastic shell ($\Delta h/h = 0$, $a_t = 22.2$ mm^2/m) and internal actions and stresses at various load levels: (a) load vs deflection; (b) cracked regions; (c) membrane forces; (d) bending moments; (e) maximum stresses in the bottom and top reinforcement layers.

a more distinct cracking phase. The concept of the cracked pseudo-ductility essentially relies on the compressive membrane actions under dead load, which ensure that the structure initially exhibits the uncracked stiffness under non-anti-funicular loading until the first section is decompressed. Figure 8a shows the load-deflection curves of synclastic shells with various degrees of double curvature, comparing their behaviour with (solid lines) and without (dotted lines) consideration of the tensile strength of the concrete. Neglecting the concrete tensile strength only slightly decreases the load in the crack formation phase, showing the dominant influence of the initial compression forces in the shell. However, the

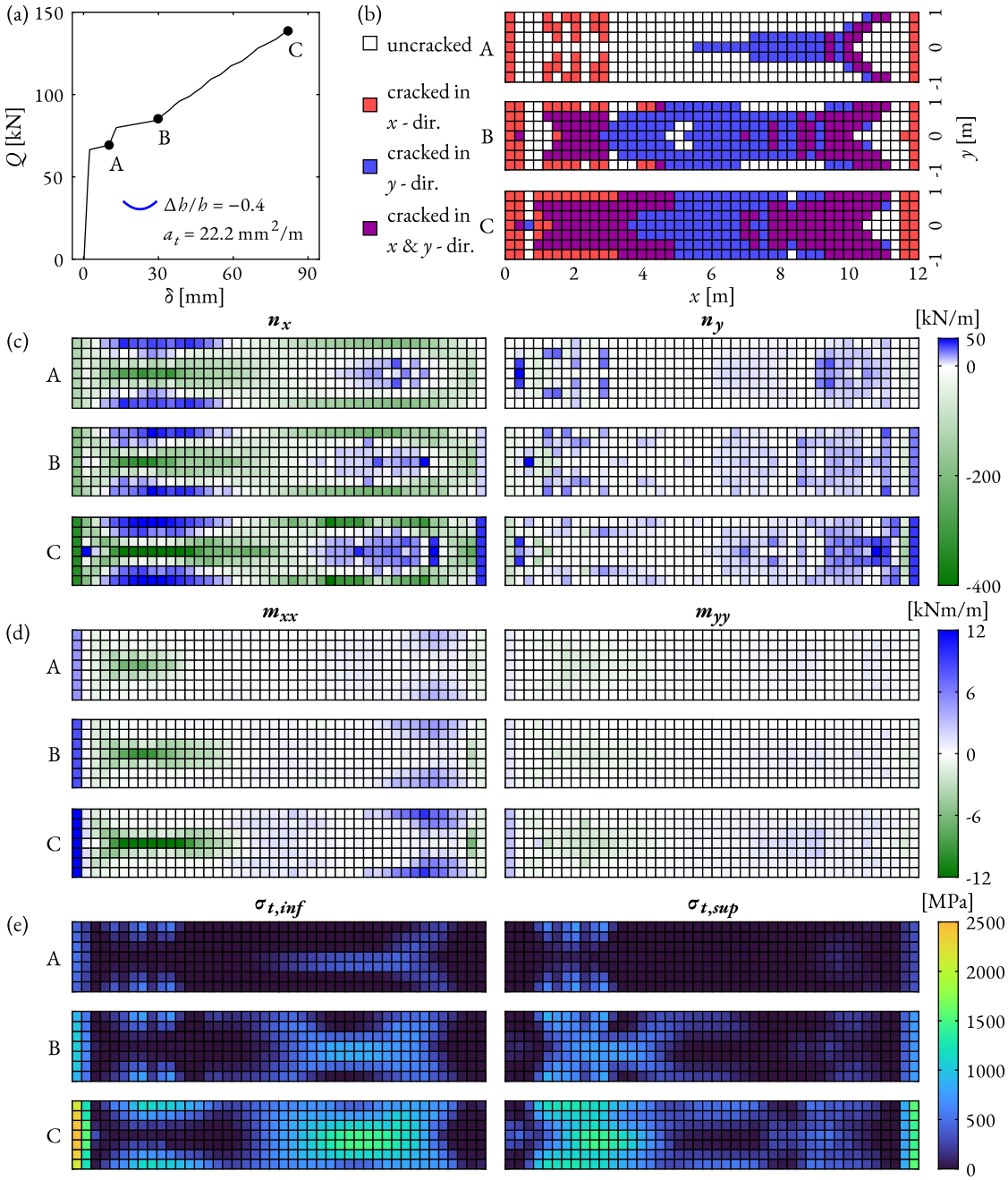

Figure 6: Load-deformation behaviour of anticlastic shell ($\Delta h/h = -0.4$, $a_t = 22.2$ mm^2/m) and internal actions and stresses at various load levels: (a) load vs deflection; (b) cracked regions; (c) membrane forces; (d) bending moments; (e) maximum stresses in the bottom and top reinforcement layers.

post-cracking behaviour reveals the profound effect of tension stiffening, which may not be neglected due to its influence on the deformation capacity and, consequently, the strength.

2.3.3. Progressive failure at ultimate load

The increase of the reinforcement ratio mainly affects the post-cracking stiffness and the failure load, as shown in the load-deflection curves of the synclastic shell in Figure 8b. Furthermore, a higher amount of reinforcement leads to a less distinct crack formation phase and a larger ratio of failure to cracking load,

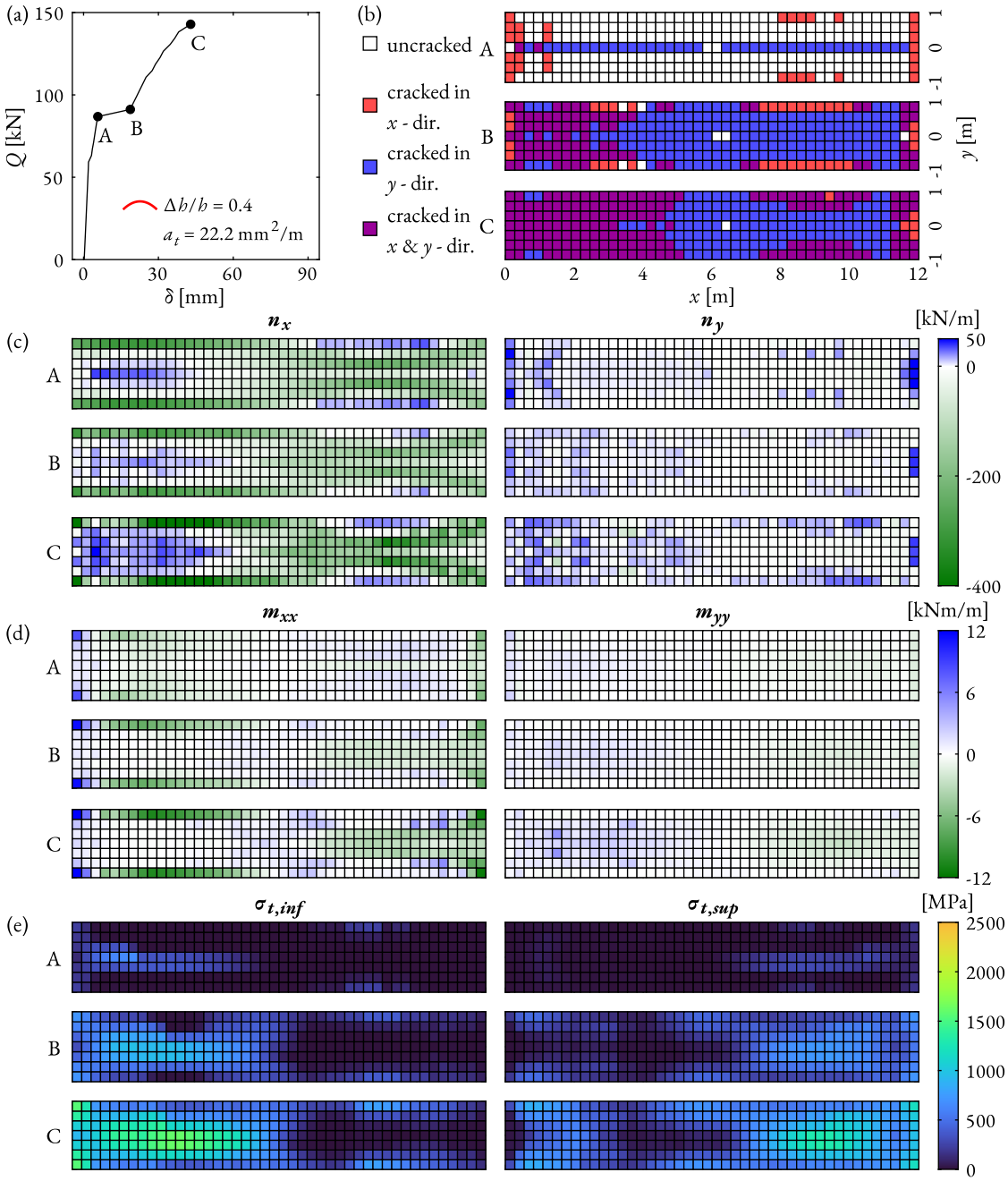

Figure 7: Load-deformation behaviour of synclastic shell ($\Delta h/h = 0.4$, $a_t = 22.2$ mm^2/m) and internal actions and stresses at various load levels: (a) load vs deflection; (b) cracked regions; (c) membrane forces; (d) bending moments; (e) maximum stresses in the bottom and top reinforcement layers.

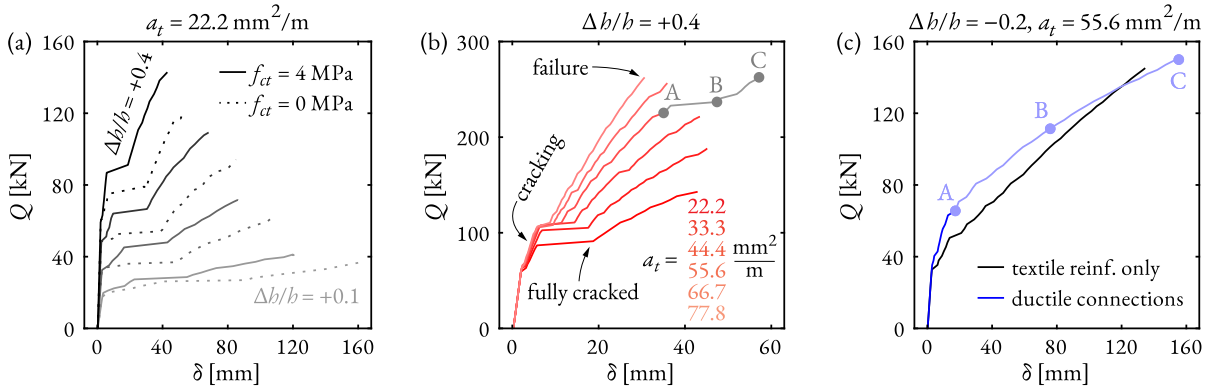

Figure 8: Load-deflection relationships of various shells, examining the influence of (a) the concrete tensile strength, (b) the reinforcement ratio, and (c) the introduction of ductile connections.

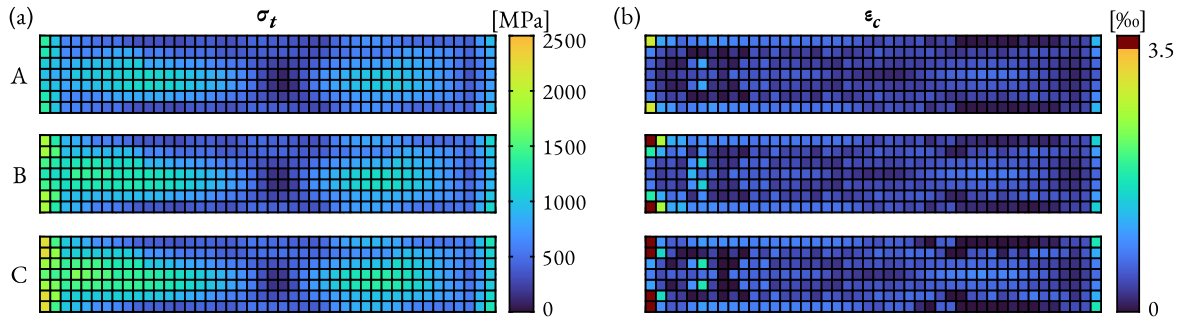

Figure 9: Behaviour of a synclastic shell after local concrete failure ($\Delta h/h = 0.4$, a_t = 55.6 mm²/m): (a) maximum tensile stresses in the textile reinforcement; (b) maximum compressive strains in the concrete. Note: rows A-C refer to the corresponding markers in Figure 8b.

which generally counters the principles regarding the announcement of an imminent collapse. The failure mode in the synclastic shells with the largest degree of double curvature is governed by the maximum admissible strain in the concrete ($\varepsilon_{cu} = -3.5‰$), while the textile reinforcement is not fully utilised yet. The behaviour of the shell after local concrete failure can be assessed when neglecting the strain limitations of the concrete. Due to the linear extrapolation of the concrete material law (Section 2.2.), the compressive stresses are zero once exceeding the strain limit, which can be interpreted as a reduction of the static depth of the shell element with the concrete failing in compression. While the resistance of the residual cross-section generally decreases, potential redistribution of the internal flow of forces – depending on the shell geometry and degree of static indeterminacy – may still enable a further load increase. This kind of behaviour is illustrated in an exemplary shell in Figure 8b, where the load increases after local concrete failure with a significantly reduced stiffness, resulting in large deformations at collapse. The corresponding maximum stresses in the textile reinforcement and strains in the concrete show that the failure is initiated in the corners of the shell in the left abutment by exceeding the strain limit of the concrete (Figure 9). The load can be further increased until, eventually, the tensile strength in the textile reinforcement is reached. Note that the crushing of the concrete leads to irreversible damage to the structure and loss of global stiffness, resulting in a limited energy dissipation potential [3].

2.3.4. Ductile connections

A ‘genuinely’ ductile behaviour in the sense of achieving plastic deformations is only feasible when introducing ductile materials to the structure. To this end, the reinforcement material is changed to a steel of class B500C (f_{sy} = 500 MPa, f_{su} = 540 MPa, and ε_{su} = 100‰) over a length of 1 m from both

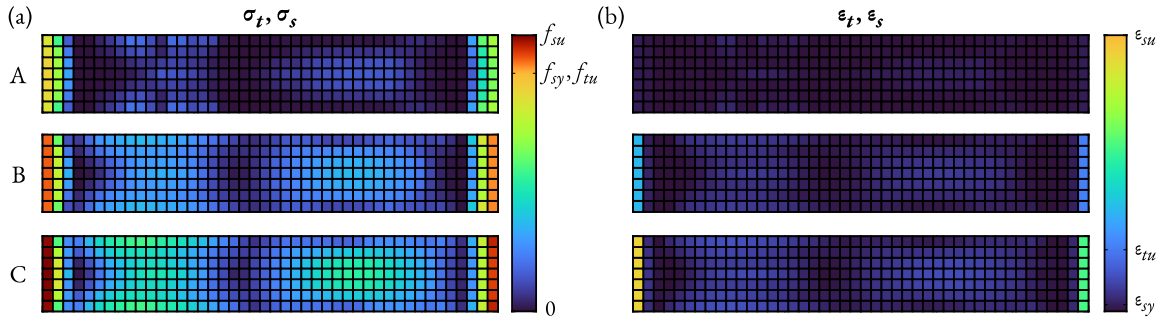

Figure 10: Yielding behaviour of an anticlastic shell ($\Delta h/h = -0.2$, $a_t = 55.6\text{mm}^2/\text{m}$): maximum tensile (a) stresses (normalised to strength) and (b) strains in the textile (σ_t, ε_t) and steel (σ_s, ε_s) reinforcement. Note: rows A-C refer to the corresponding markers in Figure 8c.

abutments of an exemplary shell ($\Delta h/h = -0.2$ and a_t = 55.6 mm^2/m), where the reinforcement area is adjusted according to the different strength of steel compared to the aramid fibres (a_s = 200 mm^2/m), with the equivalent tensile capacity being slightly smaller to provide a sufficient over-strength in the areas with brittle reinforcement materials, ensuring that the failure occurs in the plastic hinge. Figure 8c compares the load-deformation behaviour of geometrically identical shells with (blue line) and without (black line) the introduction of the ductile connections near the abutments. The shell with textile reinforcement exhibits a fairly linear increase of the load after cracking until reaching failure due to the rupture of the textile reinforcement in the left abutment. In contrast, the structural response in the post-cracking phase is initially stiffer due to the higher Young's modulus of steel (E_s = 205 GPa, E_t = 112 GPa). Once the yield strength of the reinforcement in the governing section at the left abutment is reached ('A' in Figure 8c), the global stiffness gradually decreases. After yielding, the load still significantly increases until failure due to reaching the strain limit of the steel reinforcement ($\varepsilon_{su} = 100‰$). Figure 10 illustrates the maximum utilisations of the stresses and strains in the textile and steel reinforcement in the yielding phase, showing a substantial activation of the textile reinforcement, while the stresses in the steel only slightly increase. The decrease of stiffness of the steel reinforcement in the strain hardening phase after yielding leads to a redistribution of internal forces towards the regions in the shell that exhibit a stiffer behaviour, i.e. with textile reinforcement. These results show that the mere introduction of ductile connections does not directly lead to a structural response corresponding to the ductile material behaviour but essentially depends on the shell geometry and the distribution of stiffness in the structure during the post-cracking and yielding phase.

3. Conclusions

This paper presents a case study examining various aspects of concrete shells with brittle reinforcement materials, aiming to identify the governing parameters influencing the structural response. The results obtained from the non-linear numerical simulations and the parametric study show that the introduction of double curvature significantly increases the global strength and stiffness of the examined shells since the load-bearing behaviour shifts towards a load transfer via membrane forces rather than local bending moments. While the failure behaviour is mostly brittle due to the rupture of the textile reinforcement, various means of implementing (pseudo)-ductility may still yield a benign post-cracking behaviour with sufficient stiffness at serviceability limit state while exhibiting large deformations at ultimate load, announcing the upcoming failure. The development of safe design approaches needs to consider the brittle failure mode of the textiles and potential reductions of strength due to the non-axial loading of the high-strength rovings. The design load in such structures may refer to the cracking load – comparable to the yield load in ductile elements – which is governed by the dominant compression force in the shell, while

the textile reinforcement primarily prevents the immediate collapse at cracking, potentially reducing the modelling uncertainties, which needs to be further investigated for more generalised shell geometries. The load-deformation behaviour is essentially dependent on the spatial shell geometry, presenting a further challenge for the structural design when considering higher degrees of geometric complexity and multiple load combinations. Therefore, future research may investigate the potential of inverse problems, i.e. using computational methods to determine the ideal shell geometry for given boundary conditions to achieve the desired load-bearing behaviour, which is beyond the scope of this study.

Acknowledgments

The author gratefully acknowledges Prof. Dr. Jaime Mata-Falcón (UPV) for contributing his technical expertise. This research is supported by the National Centre for Competence in Research in Digital Fabrication, funded by the Swiss National Science Foundation (project number 51NF40-141853).

References

[1] M. Popescu, "KnitCrete: Stay-in-place knitted formworks for complex concrete structures," Doctoral thesis, ETH Zürich, 2019. DOI: 10.3929/ETHZ-B-000408640.

[2] M. Popescu *et al.*, "Structural design, digital fabrication and construction of the cable-net and knitted formwork of the KnitCandela concrete shell," *Structures*, vol. 31, 2021. DOI: 10.1016/j.istruc.2020.02.013.

[3] M. Lee, "Concrete structures with stay-in-place flexible formworks and integrated textile reinforcement: An exploration of the design space and mechanical behaviour," Doctoral thesis, ETH Zürich, 2023. DOI: 10.3929/ETHZ-B-000602330.

[4] M. Lee, J. Mata-Falcón, and W. Kaufmann, "Load-deformation behaviour of weft-knitted textile reinforced concrete in uniaxial tension," *Materials and Structures*, vol. 54, no. 6, 2021. DOI: 10.1617/s11527-021-01797-5.

[5] M. Lee, J. Mata-Falcón, and W. Kaufmann, "Analysis of the tension chord in the flexural response of concrete elements: Methodology and application to weft-knitted textile reinforcement," *Engineering Structures*, vol. 261, 2022. DOI: 10.1016/j.engstruct.2022.114270.

[6] M. Lee, J. Mata-Falcón, and W. Kaufmann, "Shear strength of concrete beams using stay-in-place flexible formworks with integrated transverse textile reinforcement," *Engineering Structures*, vol. 271, 2022. DOI: 10.1016/j.engstruct.2022.114970.

[7] M. Lee, J. Mata-Falcón, M. Popescu, and W. Kaufmann, "Thin-walled concrete beams with stay-in-place flexible formworks and integrated textile shear reinforcement," *Structural Concrete*, vol. 24, no. 4, 2023. DOI: 10.1002/suco.202200648.

[8] Q. Yu, P. Valeri, M. Fernández Ruiz, and A. Muttoni, "A consistent safety format and design approach for brittle systems and application to textile reinforced concrete structures," *Engineering Structures*, vol. 249, 2021. DOI: 10.1016/j.engstruct.2021.113306.

[9] Q. Yu, M. Fernández Ruiz, and A. Muttoni, "Considerations on the partial safety factor format for reinforced concrete structures accounting for multiple failure modes," *Engineering Structures*, vol. 264, 2022. DOI: 10.1016/j.engstruct.2022.114442.

[10] M. Lee, J. Mata-Falcón, and W. Kaufmann, "Influence of short glass fibres and spatial features on the mechanical behaviour of weft-knitted textile reinforced concrete elements in bending," *Construction and Building Materials*, 2022. DOI: 10.1016/j.conbuildmat.2022.128167.